Advances in Nano Research, *Vol. 19, No. 1 (2025) 91-100*
https://doi.org/10.12989/anr.2025.19.1.091

Green synthesis of Fe_2O_3 and CuO hybrid nanoparticles and their application in one pot preparation of 3,4-dihydropyrimidin-2(1H)-thiones in water

Parisa Khodabandeh[1], Abbas Nikoo*[2] and Asghar Zamani[1,3]

[1]*Department of Nanotechnology, Faculty of Chemistry, Urmia University, Urmia, Iran*
[2]*Department of Organic Chemistry, Faculty of Chemistry, Urmia University, Urmia, Iran*
[3]*Nanotechnology Research Center, Urmia University, Urmia, Iran*

(*Received March 4, 2024, Revised July 2, 2025, Accepted July 14, 2025*)

Abstract. Maghemite (Fe_2O_3), copper oxide (CuO), and copper ferrite ($CuFe_2O_4$) nanoparticles (NPs) have been synthesized from metal nitrate and walnut shell as an inexpensive agricultural residue by a thermal decomposition method followed by open-air calcination. Also, Fe_2O_3@CuO NPs and CuO@Fe_2O_3 NPs (core/shell nanoparticles) have been synthesized by impregnation of metal oxide NPs (core) and metal nitrate solution followed by calcination. These NPs further were characterized using powder X-ray diffraction, Field emission scanning electron microscopy (FE-SEM), SEM elemental mapping, and energy dispersive X-ray spectroscopy (XRD). We find from the FESEM histograms that the average size of all pure and hybrid nanoparticles is less than 70 nm. Optimization of the reaction between benzaldehyde, thiourea and ethyl acetoacetate at mild reaction conditions in the presence of mentioned metal oxide nanomaterials revealed that CuO@Fe_2O_3NPs in water provides the best results compared to other nanomaterials. In the following, a detailed study was carried out on the Biginelli reaction with other benzaldehydes by CuO@Fe_2O_3NPs. The remarkable thing is that the catalyst is recyclable and the catalyst was reused up to five times. In reusing the catalyst, the reaction efficiency did not decrease significantly.
Keywords: copper oxide; core-shell; iron oxide; nanoparticles; topography

1. Introduction

It goes without saying that the development of technology is strongly influenced by the various applications of metal oxide nanomaterials (Mannaa *et al*. 2021, Yassin *et al*. 2023). However, at present, hybrid metal oxide nanoparticles have become a purpose of in-depth researches due to their special characteristics, because compared to simple metal oxide nanoparticles, they have many advantages, and prospects for their application are wide as well (Kannan *et al*. 2020). The various metals having dissimilar oxidation states can be used in several ratios and procedures to give hybrid metal oxide nanostructures with multi or single-phase structures (Abdelrahman and Al-Farraj 2022). In this area, various metal ferrites play a special role with their unique properties (Al-Shorifi *et al*. 2022a, b, Tobbala *et al*. 2022).

In the last two decades, due to the non-toxicity and biocompatibility of magnetite or iron oxide nanoparticles (Fe_2O_3NPs), there has been a great deal of interest for these magnetic nanomaterials in several areas such as biomedical, biosensing, energy conversion, and environmental applications (Nguyen *et al*. 2021, Ren *et al*. 2022). Furthermore, copper oxide nanoparticles (CuONPs) are one of the anticancer and antibacterial agents that also exhibit notable catalytic activity with considerable physicochemical properties (Waris *et al*. 2021, Zamani *et al*. 2021a). In addition, iron and copper oxide are inexpensive and low-toxic chemicals.

Preparation of CuO and Fe_2O_3 hybrid nanostructures in different forms provides a good chance due to the synergistic catalytic performance of Fe_2O_3 and CuO (Gao *et al*. 2020). Recently, the ability of CuO/Fe_2O_3 nanocomposites in photoelectrochemical water splitting (Kyesmen, *et al*. 2021) and the degradation of toxic pollutants (Farahani *et al*. 2022) have been considered. Also, nanostructured CuO/ Fe_2O_3 have improved ammonium perchlorate decomposition (Yang *et al*. 2023).

Biginelli reaction, which includes the condensation of urea or thiourea with ethyl acetoacetate and aldehyde derivatives, leads to the production of products with various applications. Derivatives of 3,4-dihydropyrimidin-2(1H)-thiones have properties including calcium channel modulation (Malek *et al*. 2023), α1-drenergic receptor antagonism (Majellaro *et al*. 2021), mitotic kinesin inhibition (Guido *et al*. 2015) and HIVgp-120-CD4 inhibitors (Patil *et al*. 2015). The Biginelli reaction is a three-component one-pot reaction that is carried out at high temperature. Long time and low efficiency are other disadvantages of this reaction. To reduce the time and temperature of the reaction and increase the efficiency, it is inevitable to use a catalyst. Various catalysts have been used to improve the conditions for performing the Biginelli reaction. Among the catalysts, metal oxides, including mesoporous aluminum silicate (Kamat *et al*. 2023), CeO_2 supported on poly(4-vinyl pyridine-co-divinylbenzene) (PVP-DVB)/H_2O (Shobha *et al*. 2009), $Bi_2V_2O_7$ (Sabitha *et al*. 2005), alumina supported Mo catalysts (Khademinia *et al*. 2015a), nano ZnO as a structure base catalyst (Kouachi *et al*. 2014), MnO_2–MWCNT nanocomposites (Tamaddon

*Corresponding author, Professor,
E-mail: a.nikoo@urmia.ac.ir; nikooabbas@gmail.com

ISSN: 2287-237X (Print), 2287-2388 (Online)

and Moradi *et al*. 2013), TiO_2 nanoparticles (Naik *et al*. 2009), Mg–Al–CO_3 and Ca–Al–CO_3 hydrotalcite (Lal *et al*. 2012), imidazole functionalized Fe_3O_4@SiO_2 (Javidi *et al*. 2015), Alumina supported MoO_3 (Jain *et al*. 2008), ZrO_2-pillared clay (Singh *et al*. 2006), ZnO nanoparticle (Hassanpour *et al*. 2015), Fe_3O_4-CNT (Safari and Gandomi-Ravandi 2014a), TiO_2-MWCNT (Safari and Gandomi-Ravandi 2014b), Fe_3O_4@mesoporous SBA-15 (Mondal *et al*. 2012), $Bi_2Mn_2O_7$ (Khademinia *et al*. 2015b) and RuO_2 (Soleimani *et al*. 2015), have a special place. Catalyst recycling and reuse is very important in the Biginelli reaction. If the catalyst can be recycled, it will cause the least damage to the environment and will be economically viable. The solvent and the product separation method are very important parameters in the Biginelli reaction. The water is affordable, non-toxic, available and environmentally friendly. The use of water is considered one of the important principles in green chemistry.

In the present report, a sustainable and facile technique has been investigated to synthesize a family of catalytically active pure and mixed Fe_2O_3 and CuO nanostructures. Our major method is the application of a native walnut shell as an inexpensive agricultural residue as fuel or scarified template that may highlight this technique as an ecological, harmless, and low-cost procedure (Abdollahzade and Zamani *et al*. 2023, Zamani *et al*. 2019a). Recently, we have disclosed an application of the walnut shell in the preparation of nanoceria (Zamani *et al*. 2018b), nanomagnesia (Zamani *et al*. 2019b), and nano-porous alumina and boehmite (Zamani *et al*. 2019c). Fe_2O_3 and CuO and copper iron oxide ($CuFe_2O_4$) nanoparticles (NPs) have been produced from metal nitrate and walnut shell as an inexpensive agricultural residue by a thermal decomposition method via open-air calcination. Furthermore, CuO@Fe_2O_3NPs and Fe_2O_3@CuONPs (core/shell nano-structures) have been prepared by impregnation of metal oxide NPs (core, CuO or Fe_2O_3) and metal salt solution followed by calcination. So, apart from the pure nanoparticles of Fe_2O_3 and CuO, three dissimilar types of nanoparticles including various hybrids of CuO or Fe_2O_3 were also synthesized.

It can be proposed that metal ions become distributed across the lignocellulosic matrix through interactions with the hydroxyl functional groups present in its structure (Zamani *et al*. 2019c). In this context, lignocellulose serves as a structural framework for the deposition of metal oxide precursors. Upon incorporation of metal ion species onto this biotemplate and subsequent thermal treatment, the organic framework decomposes, producing gaseous byproducts such as CO, CO_2, and H_2O. The evolution of these gases, along with the temperature rise, facilitates the formation of metal oxide nanostructures. The ultrafine nature of the resulting metal oxide can be attributed both to the templating role of lignocellulose, which guides the distribution of metal precursors, and to the release of decomposition gases, which limit particle growth and consequently lead to smaller oxide particle sizes.

In the following, the synthesis of 3,4-dihydropyrimidin-2(1H)-thiones was reported through the Biginelli condensation reaction in water at 80 °C and in the presence of prepared metal oxide NPs. Catalyst reuse, high yield of products, short reaction time, simplicity of the method, no need for a chromatography column, and easy separation are the characteristics of this method. Based on our studies, no comparative study has been conducted on the efficiency of nanoparticles of copper oxide, iron oxide and their mixture in the Biginelli reaction of thiourea.

2. Experimental

2.1 General remarks

Ferric nitrate nonahydrate, $Fe(NO_3)_2.9H_2O$, cupric nitrate hexahydrate, $Cu(NO_3)_2.6H_2O$, were purchased from Merck and used without purification. The walnut shell from a local walnut tree in Urmia, Iran was crushed using a high-speed rotary cutting mill and screened to collect the particles with a size smaller than 0.45 mm. X-ray diffraction patterns of the synthesized nanostructures obtained from Shimadzu XRD-6000 diffractometer with CuKα radiation at room temperature. The morphology and elemental observation of the nanomaterials were characterized by ZEISS Sigma 300 Field Emission Scanning Electron Microscope. The end of the reaction and the purity of 3,4-dihydropyrimidin-2(1H)-thiones were determined by thin layer chromatography (TLC). The stationary phase in thin layer chromatography (TLC) was aluminum plates coated with silica gel 60 F_{254} and the mobile phase was n-hexane/ethyl acetate (6/4) mixture. The melting point of 3,4-dihydropyrimidin-2(1H)-thiones was measured by open capillary on Electrothermal 9200.

2.2 Preparation of metal oxide nanoparticles

Pure nanoparticles (CuONPs and Fe_2O_3NPs) were prepared using the following procedure. Initially, in 100mL of deionized water (Millipore, Milli-Q grade) 10 g of walnut shell and 6.9 mmol of corresponding metal nitrate were mixed at room temperature. After 5 h stirring, the water of the resulting mixture was removed through evaporation under reduced pressure and the resulting solid was calcined at 500 °C for 4 h under open-air conditions. By the same method but using 6.9 mmol $Fe(NO_3)_2.9H_2O$ and 3.45 mmol $Cu(NO_3)_2.6H_2O$, $CuFe_2O_4$ nanoparticles ($CuFe_2O_4$NPs) can be produced. Also, CuO@Fe_3O_4NPs and Fe_2O_3@CuONPs (core/shell nanoparticles) have been prepared by impregnation of CuONPs or Fe_2O_3NPs (core) and metal nitrate solution (molar ratio of metal in core to metal nitrate: 1:1) and the resulting solid was calcined at the same conditions.

2.3 General procedure for the synthesis of 3,4-dihydropyrimidin-2(1H)-thiones

Thiourea (7.5 mmol, 750.9 mg), ethyl acetoacetate (5 mmol, 650 mg), aldehyde derivatives (5 mmol), metal oxide nanocatalyst and water 50 ml were added in a round-bottomed flask equipped with a condenser and a magnetic stirrer. The contents of the flask were stirred at 80°C. The

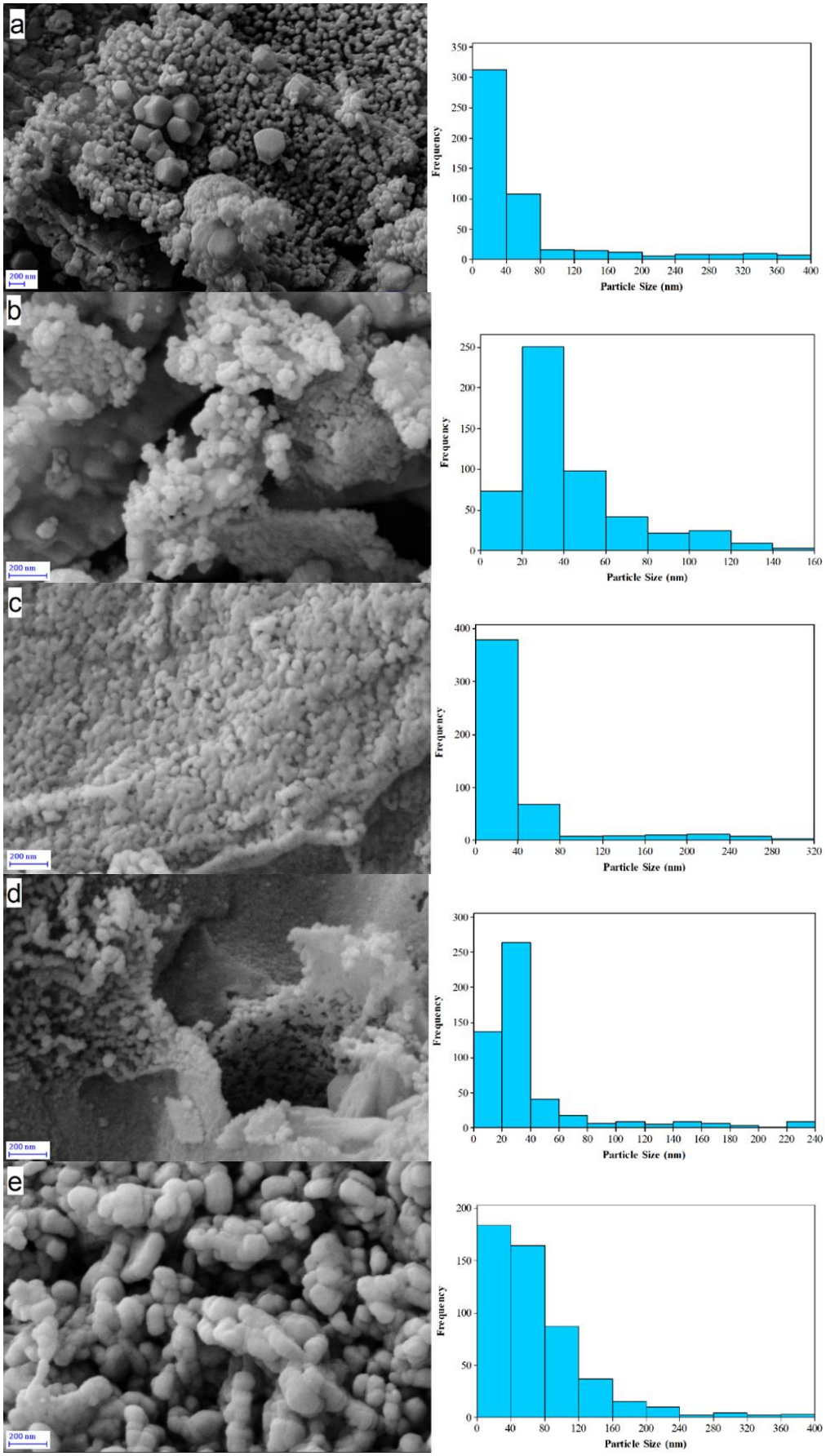

Fig. 1 FESEM images and size distribution of a) CuONPs, b) Fe_2O_3 NPs, c) $CuFe_2O_4$ NPs, d) CuO@Fe_2O_3NPs, and e) Fe_2O_3@CuO NPs

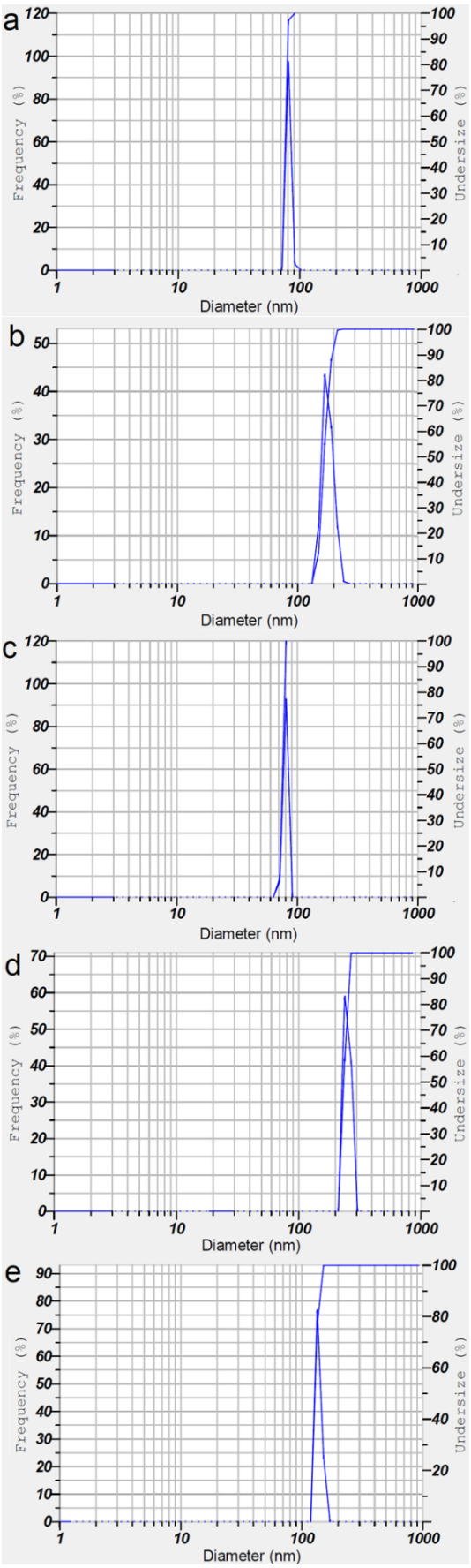

Fig. 2 Dynamic Light Scattering analysis of a) CuONPs, b) Fe_2O_3 NPs, c) $CuFe_2O_4$ NPs, d) $CuO@Fe_2O_3$NPs, and e) Fe_2O_3@CuO NPs

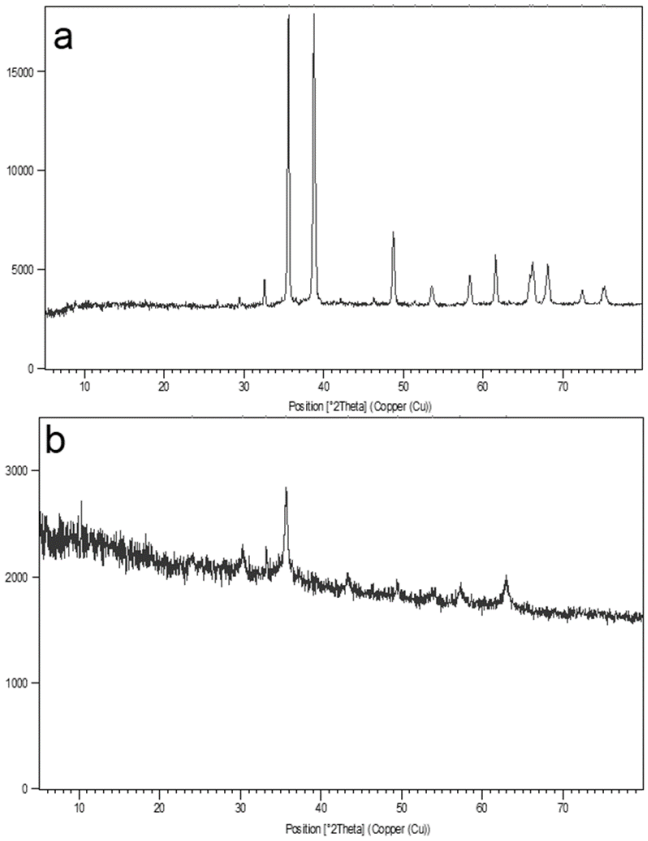

Fig. 3 XRD pattern of a) CuONPs, and b) Fe_2O_3 NPs

progress of the reaction was monitored by thin layer chromatography (TLC) with mobile phase n-hexane/ethyl acetate (6/4) mixture. After the completion of the reaction, the reaction mixture was cooled to room temperature. 3,4-dihydropyrimidin-2(1H)-thiones was extracted by ethyl acetate (3×25 ml). After dissolving ethyl acetate by rotary, 3,4-dihydropyrimidin-2(1H)-thiones was crystallized in ethanol. After extraction of 3,4-dihydropyrimidin-2(1H)-thiones, the reaction residue was filtered and the precipitates obtained were washed with acetone (3×25 ml). The nanocatalysts were dried at 80°C for 2 hours and reused for the next reaction.

3. Results and discussion

3.1 Characterization of metal oxide nanoparticles

Figs. 1a-e show SEM images of metal oxide nanomaterials, as well as size distributions deduced from SEM images. The reported mean diameter by scanning electron microscopy of the spherical nanoparticles were 72 nm, 43 nm, 50 nm, 44nm, 74 nm for CuONPs, Fe_2O_3NPs, $CuFe_2O_4$NPs, $CuO@Fe_2O_3$NPs, and Fe_2O_3@CuONPs, respectively. Also, SEM images show mainly spherical nanoparticles but with various aggregation modes in all of the studied samples. It should be mentioned that compared to the methods in which agricultural wastes and fruit peels are used (Mussttaf *et al*. 2024) for the synthesis of iron and copper oxide nanoparticles and their mixtures, it can be said

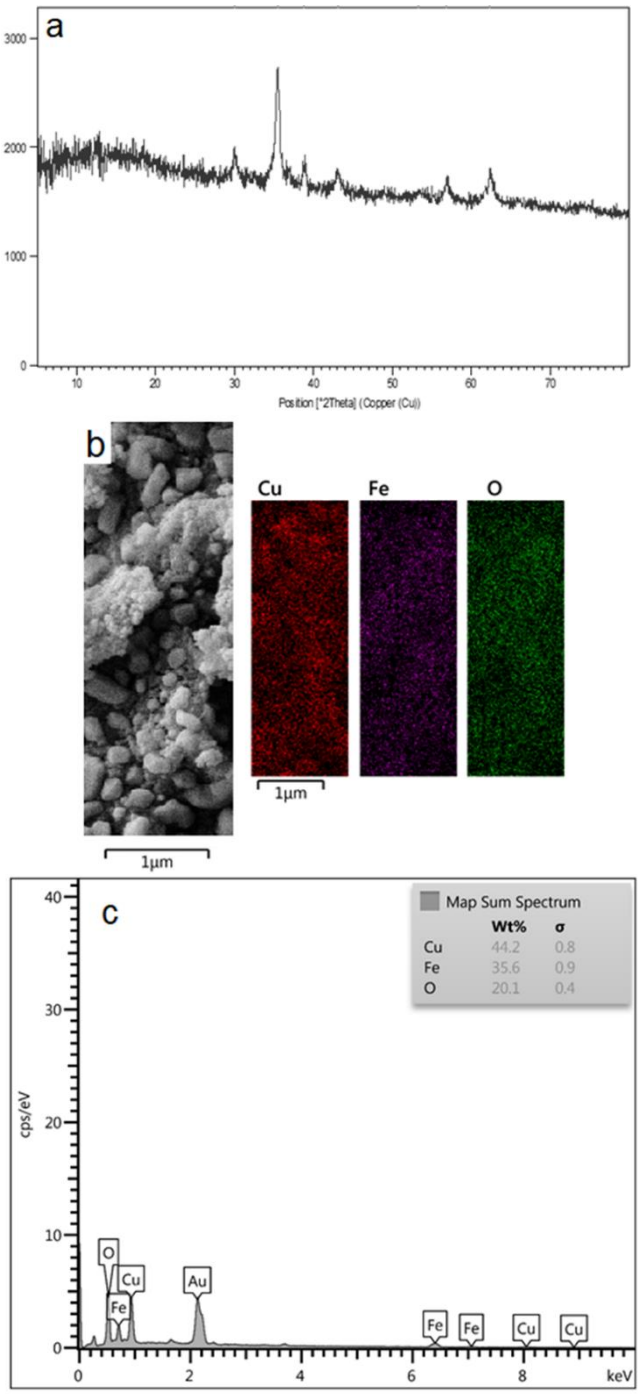

Fig. 4 a) XRD pattern, b) SEM mapping images, and c) EDX of $CuFe_2O_4$ NPs

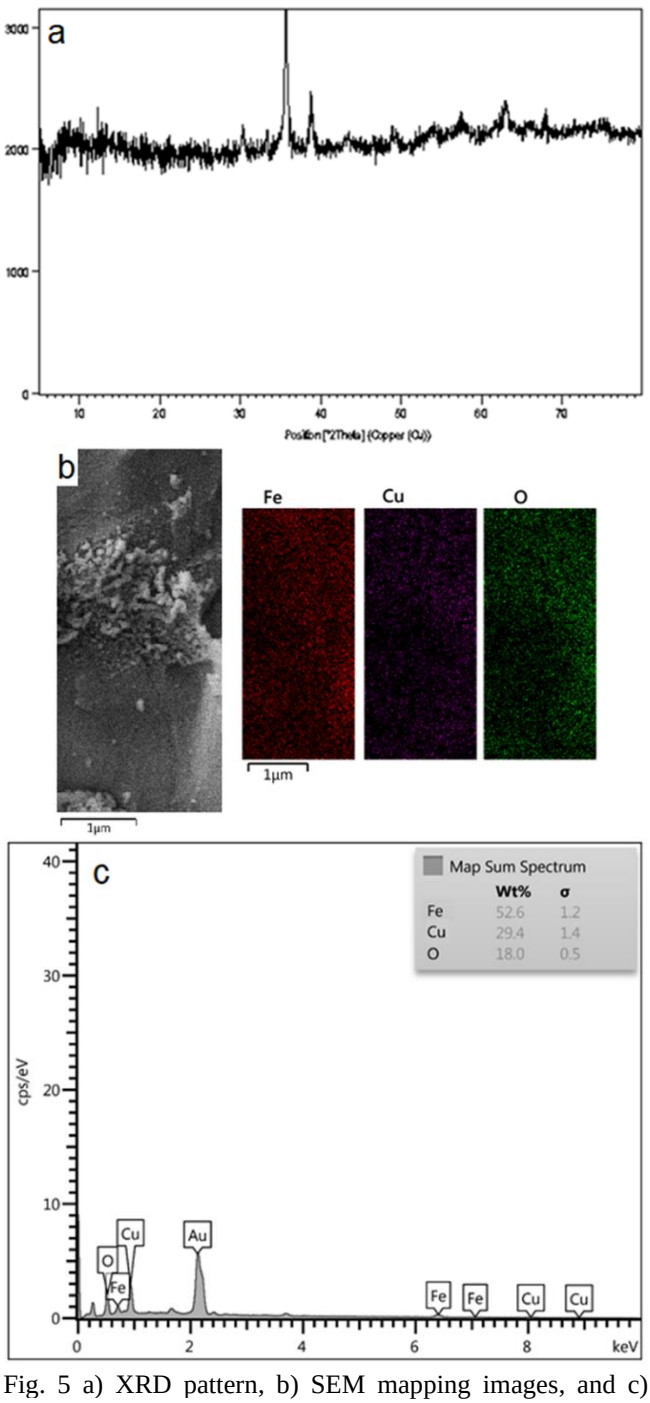

Fig. 5 a) XRD pattern, b) SEM mapping images, and c) EDX of CuO@Fe_2O_3NPs

that in our method, in addition to the simplicity of the method, the size of the synthesized nanoparticles is clearly smaller.

As can be seen, the size of the particles obtained from DLS analysis is much larger than the size obtained using the FESEM histogram (Fig. 2). This difference is due to the principle that the DLS technique provides the hydrodynamic diameter of agglomerated particles rather than the real size of nanoparticles (Ma *et al*. 2012).

X-ray diffraction (XRD) analysis of synthesized different metal oxide nanostructures were shown in Fig. 3a. The XRD pattern in Fig. 3a matched with the monoclinic structure of CuO crystal (JCPDS card 80-1917). An intense diffraction peak at 38.76 was detected corresponding to the lattice plane (111). Likewise, several other extra at 35.55 (002) and 48.72 (202), were also observed. Fig. 3b showed a series of diffraction peaks at 2θ of 23.95, 33.18, 35.63, 49.44, 53.84, 57.26 and 62.88 can be attributed to (012), (104), (110), (024), (116), (122) and (214) planes, respectively. This XRD pattern was indexed to the rhombohedral phase of alpha-hematite or α-Fe_2O_3 (JCPDS card 24-0072).

Fig. 4a shows the XRD pattern of the $CuFe_2O_4$. In the XRD spectrum of $CuFe_2O_4$, the diffraction peaks at 2θ =

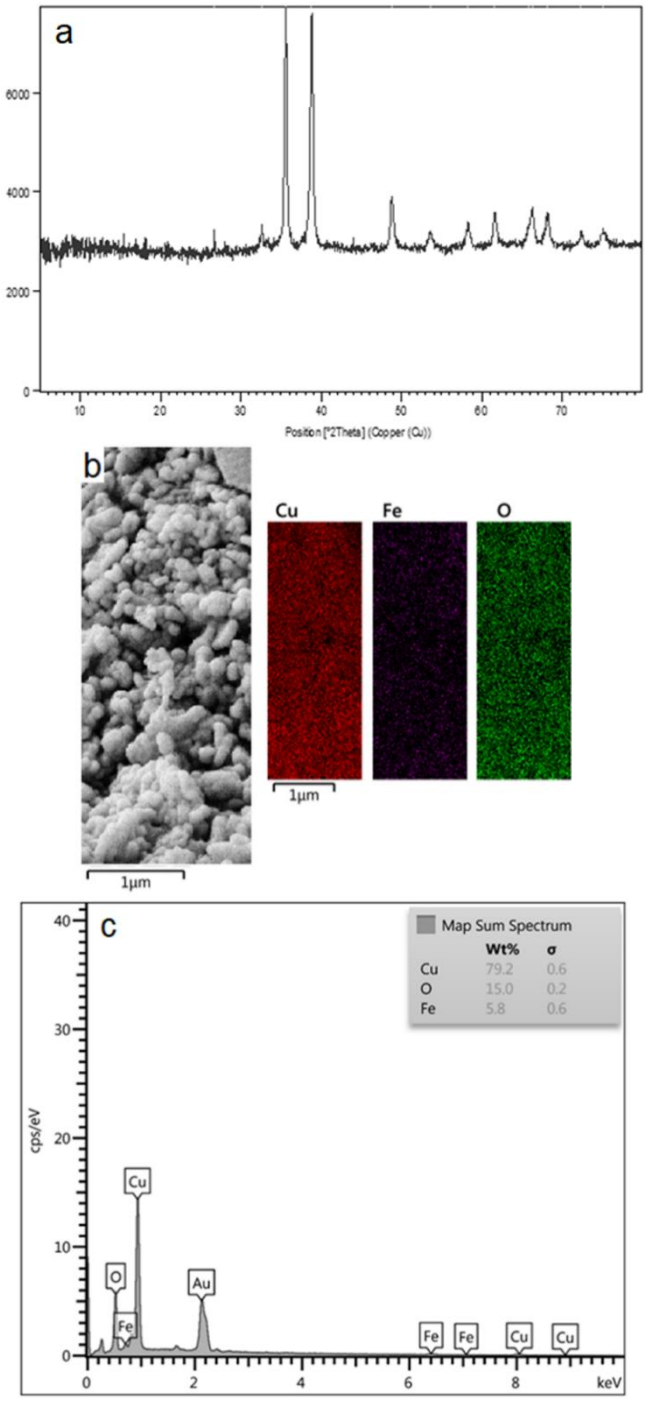

Fig. 6 a) XRD pattern, b) SEM mapping images, and c) EDX of Fe_2O_3@CuO NPs

Table 1 Crystalographical data, SEM and DLS based diameter of metal oxide nanomaterials

Nanomaterial	Peak position 2θ (°)	FWHM (°)	Crystallite size D (nm)	SEM diameter (nm)	DLS diameter (nm)
CuONPs	38.76	0.24	38	72	76
Fe_2O_3NPs	35.63	0.40	23	43	168
$CuFe_2O_4$NPs	35.42	0.61	15	50	76
CuO@Fe_2O_3NPs	35.67	0.41	22	44	230
Fe_2O_3@CuONPs	38.77	0.36	25	74	130

29.99, 35.42, 43.06, 56.87, and 62.34 could be indexed to the (220), (311), (400), (511), and (440) planes of cubic spinel $CuFe_2O_4$ (JCPDS card 06-0545). Also, The diffraction peak at diffraction angle 2θ = 38.81 can be related to CuO. As illustrated in Fig. 4b SEM mapping images of Cu, Fe and O elements in the $CuFe_2O_4$NPs confirmed higher contrast distribution of Cu element which can be consistent with the formation of CuO and $CuFe_2O_4$ that was also observed in the XRD pattern Fig. 4a. This information, along with the EDX elemental analysis (Fig. 4c), shows that in sample $CuFe_2O_4$ NPs, some Fe_2O_3 particles were also produced, which were coated by CuO and $CuFe_2O_4$NPs.

The CuO@Fe_2O_3NPs XRD pattern in Fig. 5a revealed diffraction peaks at 35.67 (stronger peak) and 38.79 (weaker peak) which were related to the Fe_2O_3 and CuO respectively, which confirms the core (CuO)/ shell (Fe_2O_3) structure. XRD pattern along with SEM mapping images (Fig. 5b) and EDX elemental analysis (Fig. 5c) confirm the core shell structure of CuO@Fe_2O_3NPs. As is clear, Fig. 3b shows a higher contrast distribution of Fe element in the shell.

Also, The Fe_2O_3@CuO NPs XRD pattern in Fig. 6a revealed diffraction peaks at 35.56 and 38.77 which were related to CuO layer. XRD pattern along with SEM mapping images (Fig. 6b) and EDX elemental analysis (Fig. 6c) confirm core shell structure of Fe_2O_3@CuONPs. As is clear, SEM mapping images Fig. 4b show a higher contrast distribution of Cu element in the shell.

The crystallite sizes of grains were determined through Debye Scherrer formula and full-width half maximum (FWHM) of the most intense peak.

$D = k\lambda / \beta\cos\theta$ Debye Scherrer formula

Where k = 0.**89**, 'D' represents the average crystallite size (nm), λ is the wavelength of X-ray (0.15406 nm) and β constitutes the FWHM.

Regarding the possible mechanism of the formation of CuONPs, Fe_2O_3NPs and $CuFe_2O_4$NPs metal oxide nanomaterials, it can be said that, it is conceivable that the metal ions were dispersed on Lignocellulosic biomass (walnut shell) via coordination with their hydroxyl groups. Therefore, lignocellulosic component act as a template for the metal precursors. After dispersion of the metal ions on the template and increasing of the temperature, the template and nitrate were removed by transformation into CO, CO_2, NO_2 and H_2O. Simultaneously with gas release from the template, metal nanoparticles is formed due to temperature increase. Also, The purity of nanomaterials has been investigated by atomic absorption.

To prepare core-shell nanoparticles, by adding metal nitrate to metal oxide nanoparticles and removing water, the metal nitrate is distributed and absorbed on the surface of the monometal oxide, and then by calcining the resulting mixture, a layer of new metal oxide is formed on the previous metal oxide nanoparticles.

3.2 Catalytic activity

The catalytic activity of monometal (Fe_2O_3NPs and CuONPs) and bimetal ($CuFe_2O_4$NPs, Fe_2O_3@CuONPs and

Table 2 Optimization of catalyzed synthesis of 3,4-dihydro-pyrimidin-2(1H)-thione

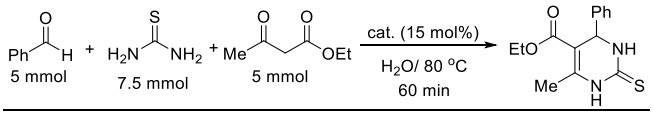

Entry	Catalyst	Yields (%)
1	-	8.6
2	CuONPs	28.3
3	Fe_2O_3NPs	13.7
4	Fe_2CuO_4NPs	64.2
5	CuO@Fe_2O_3NPs	95
6	Fe_2O_3@CuONPs	74.5

Table 3 Optimization of amount of the catalyst CuO@Fe_2O_3NPs on the synthesis of 3,4-dihydropyrimidin-2-thione

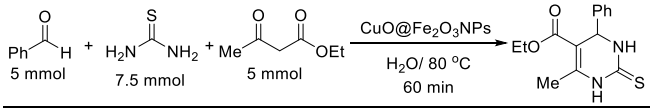

Entry	Catalyst (mol%)	Yields (%)
1	10	53
2	15 (120 mg)	95
3	20	59
4	25	58
5	50	50

Table 4 Synthesis of 3,4-dihydropyrimidin-2-thione derivatives

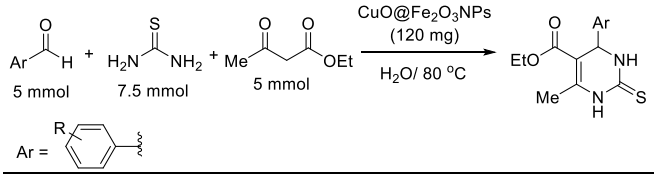

Entry	R	Time (min)	Yield (%)	Melting point (°C)	
				Found	Reported
1	H	60	95	207-209	208-210
2	4-Me	100	88	193-195	192-194
3	4-MeO	120	85	150-152	152-154
4	2-HO	70	89	241-243	240-242
5	3-HO	60	92	180-182	183-185
6	4-HO	90	86	224-226	220-222
7	2-O_2N	60	87	214-216	215-217
8	3-O_2N	45	90	206-608	208-210
9	4-O_2N	35	95	204-206	206-208
10	2-Cl	50	87	218-220	219-221
11	4-Cl	45	96	190-192	188-190
12	2,4-diCl	50	91	220-222	225-227

CuO@Fe_2O_3ONPs) oxide nanoparticles was first investigated using a three-component Biginelli reaction. The experimental setup for the Biginelli reaction involves a round-bottom flask equipped with a magnetic stirrer and, a reflux condenser. Into the flask, benzaldehyde, ethyl acetoacetate, and thiourea are added in stoichiometric amounts, in water as solvent. Nanocatalysts is introduced to promote the reaction. The mixture is stirred and heated to 80 °C. Reaction progress is monitored via TLC. After completion, the reaction mixture is cooled, and the product typically precipitates. Finally, the product is dried and characterized using techniques like NMR and melting point analysis.

Regular investigations were carried out to find the type of metal oxide nanostructures as catalyst (Table 2). To find the optimal reaction conditions, we performed a reaction of benzaldehyde, ethylacetoacetate and thiourea as a model reaction at 80 °C in aqueous media. While entry 1 from table 2 proves the importance of presence the catalyst in this reaction, our studies revealed that among monometal ($Fe_{32}O_3$NPs and CuONPs) and bimetal ($CuFe_2O_4$NPs, Fe_2O_3@CuONPs and CuO@Fe_2O_3ONPs) oxide nano-particles used in the reaction, bimetal oxide nanoparticles had resulted in the highest product yields (Table 2, entries 4-6). The results point out the synergetic effect of bimetal oxide catalysts in comparison to the Fe_2O_3NPs and CuONPs. The best performance was attained with CuO@Fe_2O_3 catalyst achieving 95% of the product. As can be seen, among the three bimetallic catalysts, the catalysts containing core/shell structures (Fe_2O_3@CuONPs and CuO@Fe_2O_3ONPs) have shown better performance than $CuFe_2O_4$NPs, which may be due to the amorphous nature of these two catalysts and as a result of increasing their catalytic properties (Yoon and Cocke 1986).

In the next stage, we focused on the effect of the amount of the catalyst CuO@Fe_2O_3NPs on the synthesis of 3,4-dihydropyrimidin-2(1H)-thione (Table 3) and it was found that 15 mol% of the catalyst is very suitable for carrying out the reaction (Table 3, entry 2). It is necessary to mention, the yield of the product was reduced to 50-95 by further increasing in quantity of catalyst (Table 3, entries 3-5). The observed decrease in yield at higher catalyst loadings can be attributed to multiple interrelated factors. Excessive amounts of solid nanostructured catalyst may lead to mass transfer limitations due to increased viscosity or reduced substrate diffusion. Additionally, higher concentrations can promote nanoparticle agglomeration, thereby reducing the available active surface area. Overloading may also impair proper mixing and heat distribution within the reaction medium, negatively affecting reaction kinetics and overall efficiency (Liu *et al*. 2009).

Under these optimized process conditions, the reaction between several benzaldehydes, ethyl acetoacetate and thiourea was subsequently applied in water at 80 °C in the presence of CuO@Fe_2O_3NPs as the catalyst (Table 4). It is also clear from the tabulated results, that either electron-poor or-rich benzaldehydes reacted well under the reaction conditions to attain the corresponding dihydropyrimidinones in high-to-quantitative yields with high purity. Electron-rich benzaldehydes containing 4-methyl or 4-methoxy (Table 4, entries 2-4, 6) substituents react at a slower rate than benzaldehyde, and on the contrary, electron-deficient benzaldehydes containing nitro or chloro substituents react at a faster rate than benzaldehyde (Table 4, entries 8-12). It

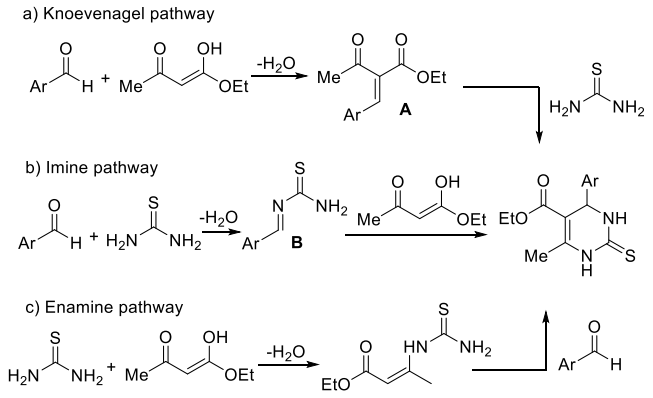

Scheme 1 The Suggested mechanisms for synthesis of 3,4-dihydropyrimidin-2(1H)-thiones

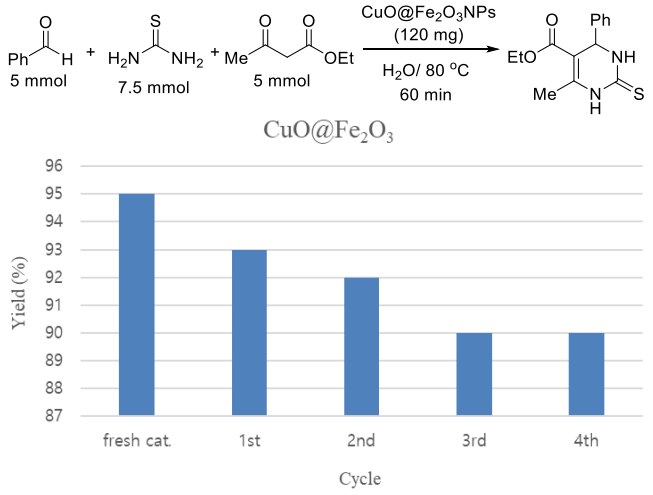

Scheme 2 Reusability of catalyst $CuO@Fe_2O_3$

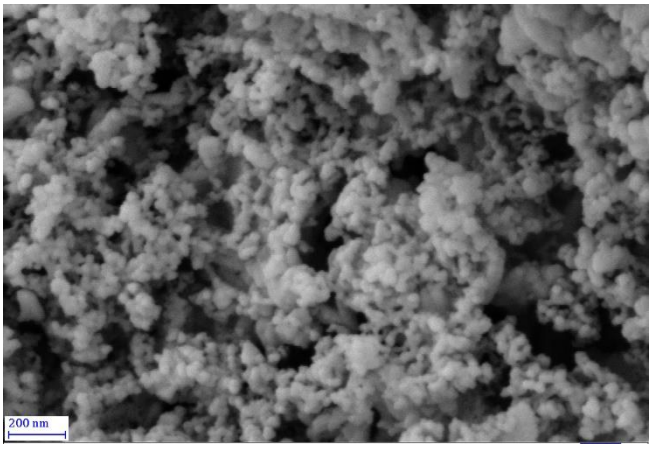

Fig. 7 SEM image of $CuO@Fe_2O_3$NPs after 5th recycling

should be noted that the comparison of entries 4 and 6 gives good information about the mechanism. As expected, the electron-rich reagents such as 4-hydroxybenzaldehyde participate in the reaction at a slower rate, but based on the electronic properties, the same is expected from the 2-hydroxybenzaldehyde. However, the latter reagent shows more reactivity than 4-hydroxybenzaldehyde. The reason for this observation can be found in the chelating ability of 2-hydroxybenzaldehyde-based Schiff base (Parambadath *et al*. 2020) intermediate **B** for metal ions (Scheme 1). Therefore, considering the three main proposed pathways as the mechanism of the Biginelli reaction, it can be said that our proposed mechanism in the current research is the imine pathway.

The $CuO@Fe_2O_3$NPs catalyst was chosen as the best catalyst, due to its aforesaid characteristics, its recyclability was examined over five continual runs. The recovered catalyst was successfully used in four subsequent reactions and exhibited consistent catalytic activity without a significant loss of its catalytic activity (Scheme 2). Also, the SEM image of the catalyst after 5 times of recycling (Fig. 7) shows that there was no significant change in the size of the nanoparticles and therefore no significant change was seen in the efficiency of the recycled catalyst.

Based on the investigations, most of the methods that have been presented in the field of Biginelli reaction by thiourea have been done in ethanol as a solvent and in relatively long times (Chandravarkar *et al*. 2023). But according to our method, this reaction can be done in water solvent in 35-120 minutes.

It should be noted that the present method offers a more cost-effective and facile approach compared to other strategies that rely on expensive catalysts such as praseodymium (III) nitrate (Stiti *et al*. 2025) or those that require complex and multi-step synthesis procedures nitrate (Taravati *et al*. 2025). Moreover, unlike many conventional methods, this approach avoids the use of environmentally hazardous reagents and eliminates the need for harsh acidic (Bouafina *et al*. 2025**)** conditions, making it both eco-friendly and operationally simpler.

4. Conclusions

Pure nanoparticles Fe_2O_{43}NPs and CuONPs, and also copper ferrite, $CuFe_2O_4$NPs were successfully prepared by adsorption of metal ions on inexpensive agricultural residue, walnut shell and calcination under open-air conditions without using any precipitating agents, stabilizer or controlling *p*H. In the following step, $CuO@Fe_2O_3$NPs and $Fe_2O_3@$CuONPs (core/shell nanostructures) have been produced by impregnation of metal oxide nanoparticles as core and metal ion aqueous solution followed by calcination. Nanomaterials were characterized by XRD, FESEM, and EDX. The prepared nanometal oxides were used as heterogeneous catalysts for the synthesis of 3,4-dihydropyrimidin-2(1H)-thiones. It was found that $CuO@Fe_2O_3$ nanocatalyst performs better for the synthesis of 3,4-dihydropyrimidin-2(1H)-thiones. One of the features of the present work was the use of water as a green solvent under 80 °C. Performing the reaction in a short time with high efficiency is one of the important points of this method. Another feature of the present work is the possibility of reusing the catalyst without significantly reducing the product efficiency.

Our findings show that it is possible to synthesize nanostructures containing different mixtures of metal oxides in a simple, green and cost-effective way, and these mixed metal oxide nanostructures can provide different catalytic results than monometal oxide nanoparticles. The investigation of synergistic effects in mixed metal oxides in catalytic

reactions can lead to the creation of a new generation of catalysts in the field of production of fine and bulk chemicals.

Acknowledgments

The authors gratefully acknowledge the financial support for this work by the research council of Urmia University.

References

Abdelrahman, E.A. and Al-Farraj, E.S. (2022), "Facile synthesis and characterizations of mixed metal oxide nanoparticles for the efficient photocatalytic degradation of rhodamine b and congo red dyes", *Nanomaterials*, **12**(22), 3992. https://doi.org/10.3390/nano12223992.

Abdollahzade, H., Zamani, A. (2023), "Recent developments in liquid-phase synthesis and applications of nanomagnesia", *Adv. Nano Res.*, 14(1), 103-115. https://doi.org/10.12989/anr.2023.14.1.103.

Alshorifi, F.T., Ali, S.L. and Salama, R.S. (2022a), "Promotional Synergistic Effect of Cs–Au NPs on the Performance of Cs–Au/$MgFe_2O_4$ Catalysts in Catalysis 3,4-Dihydropyrimidin-2(1H)-Ones and Degradation of RhB Dye", *J. Inorg. Organomet. Polym.*, **32**, 3765-3776. https://doi.org/10.1007/s10904-022-02389-8a.

Al-Shorifi F.T., Alswat, A.A. and Salama, R.S. (2022b), "Gold-selenide quantum dots supported onto cesium ferrite nano-composites for the efficient degradation of rhodamine B", *Heliyon*. **8**(6), e29371. https://doi.org/10.1016/j.heliyon.2022.e09652.

Bouafina, K., Belferdi, F. and Bouremmad, F. (2025), "Sufonated biochar derived from eucalyptus bark as natural catalyst in the biginelli reaction" *Russ. J. Gen. Chem.*, **95**(3), 1-8. https://doi.org/10.1134/S1070363224613048.

Chandravarkar, A., Aneeja, T. and Anilkumar, G. (2023), "Advances in Biginelli reaction: A comprehensive review" *J. Heterocyclic Chem.*, **61**(1), 1-24. https://doi.org/10.1002/jhet.4742.

Farahani, A.T., Goodarzi, M. and Hedayati, K. (2022), "Synthesis of γ-Fe_2O_3-CuO nanocomposite: structural and magnetic study and its application for degradation of toxic pollutants", *J. Mater. Sci. Mater. Electr.*, **33**, 23761-23769. https://doi.org/10.1007/s10854-022-09134-4.

Gao, Y., Zhang, N., Wang, C., Zhao, F. and Yu, Y. (2020), "Construction of Fe_2O_3@CuO Heterojunction Nanotubes for Enhanced Oxygen Evolution Reaction", *ACS Appl. Energy Mater.*, **3**(1), 666-674. https://doi.org/10.1021/acsaem.9b01866.

Guido, B.C., Ramos, L.M., Nolasco, D.O., Nobrega, C.C. andrade, B.Y.G., Pic-Taylor, A., Neto, B.A.D. and Corrêa J.R. (2015), "Impact of kinesin Eg5 inhibition by 3,4-dihydropyrimidin-2(1H)-one derivatives on various breast cancer cell features", *BMC Cancer*, **15**, 283. https://doi.org/10.1186/s12885-015-1274-1.

Hassanpour, A., Hosseinzadeh Khanmiri, R. and Abolhasani, J. (2015), "ZnO nanoparticles as an efficient, heterogeneous, reusable, and ecofriendly catalyst for one-pot, three-component synthesis of 3,4-Dihydropyrimidin-2(1H)-(thio)one Derivatives in water", *Synth. Commun.*, **45**(6), 727-733. https://doi.org/10.1080/00397911.2014.987350.

Jain, S.L., Prasad, V.V.D.N. and Sain, B. (2008), "Alumina supported MoO_3: An efficient and reusable heterogeneous catalyst for synthesis of 3,4-dihydropyridine-2(1H)-ones under solvent free conditions", *Catal. Commun.*, **9**(4), 499-503. https://doi.org/10.1016/j.catcom.2007.04.021.

Kamat, V., Reddy, D.S. and Kumar A. (2023), "Catalytic role in Biginelli reaction: Synthesis and biological property studies of 2-oxo/thioxo-1,2,3,4-tetrahydropyrimidines", *Arch. Pharm.* **356**(6), 2300008. https://doi.org/10.1002/ardp.202300008.

Javidi, J., Esmaeilpour, M. and Nowroozi Dodeji, F. (2015), "Immobilization of phosphomolybdic acid nanoparticles on imidazole functionalized Fe_3O_4@SiO_2: A novel and reusable nanocatalyst for one-pot synthesis of Biginelli-type 3,4-dihydro-pyrimidine-2-(1H)-ones/thiones under solvent-free conditions", *RSC Adv.*, **5**, 308-315. https://doi.org/10.1039/C4RA09929J.

Kannan, K., Radhika, D., Sadasivuni, K.K., Reddy, K.R. and Raghu, A.V. (2020), "Nanostructured metal oxides and its hybrids for photocatalytic and biomedical applications", *Adv. Colloid Interface Sci.*, **281**, 102178. https://doi.org/10.1016/j.cis.2020.102178.

Khademinia, S., Behzad, M., Alemi, A., Dolatyari, M. and Sajjadi S.M. (2015b), "Catalytic performance of bismuth pyromanganate nanocatalyst for Biginelli reactions" *RSC Adv.*, **5**, 71109-71114. https://doi.org/10.1039/C5RA11432B.

Khademinia, S., Behzad, M. and Jahromi, H.S. (2015a), "Solid state synthesis, characterization, optical properties and cooperative catalytic performance of bismuth vanadate nanocatalyst for biginelli reactions", *RSC Adv.*, **5**, 24313. https://doi.org/10.1039/C5RA00368G.

Kouachi, K., Lafaye, G., Pronier, S., Bennini, L. and Menad, S. (2014), "Mo/γ-Al_2O_3 catalysts for the Biginelli reaction. Effect of Mo loading", *J. Mol. Catal. A Chem.*, **395**, 210-216. https://doi.org/10.1016/j.molcata.2014.08.025.

Kyesmen, P.I., Nombona, N. and Diale, N. (2021), "Heterojunction of nanostructured α-Fe_2O_3/CuO for enhancement of photoelectrochemical water splitting", *J. Alloys Compd.*, **863**, 158724. https://doi.org/10.1016/j.jallcom.2021.158724.

Lal, J., Sharma, M., Gupta, S., Parashar, P., Sahu, P. and Agarwal, D.D. (2012), "Hydrotalcite: A novel and reusable solid catalyst for one-pot synthesis of 3,4-dihydropyrimidinones and mechanistic study under solvent free conditions", *J. Mol. Catal. A Chem.*, **352**, 31-37. https://doi.org/10.1016/j.molcata.2011.09.009.

Liu, J., Qiao, S.Z., Hu, Q.H. and Lu, G.Q. (2009), "Magnetic nanocomposites with mesoporous structures: synthesis and applications", *Small*, **5**(4), 425-443. https://doi.org/10.1002/smll.200801595.

Ma, R., Levard, C., Marinakos, S.M., Cheng, Y., Liu, J., Michel, F.M., Brown, G.E., Lowry, G.V. (2012), "Size-controlled dissolution of organic-coated silver nanoparticles", *Environ. Sci. Technol.*, **46**(2), 752-759. https://doi.org/10.1021/es201686j.

Majellaro, M., Jespers , W., Crespo , A., Núñez , M.J., Novio , S., Azuaje , J., Prieto-Díaz , R., Gioé , C., Alispahic , B., Brea , J., Loza, M.I., Freire-Garabal, M., Garcia-Santiago, C., Rodríguez-García, C., García-Mera, X., Caamaño, O., Fernandez-Masaguer, C., Sardina, J.F., Stefanachi, A., El Maatougui, A., Mallo-Abreu, A., Åqvist, J., Gutiérrez-de-Terán, H. and Sotelo, E. (2021), "3,4-Dihydropyrimidin-2(1 H)-ones as Antagonists of the Human A2B Adenosine Receptor: Optimization, structure-activity relationship studies, and enantiospecific recognition", *J. Med. Chem.*, **64**(1), 458-480. https://doi.org/10.1021/acs.jmedchem.0c01431.

Malek, R., Simakov, A., Davis, A., Maj, M., Bernard, P.J., Wnorowski, A., Martin, H., Marco-Contelles, J., Chabchoub, F., Dallemagne, P., Rochais, C., Jozwiak, K. and Ismaili, L. (2023), "Biginelli reaction synthesis of novel multitarget-directed ligands with Ca^{2+} channel blocking ability, cholinesterase inhibition", antioxidant capacity, and Nrf2 activation", *Molecules*, **28**(1), 71. https://doi.org/10.3390/molecules28010071.

Mannaa, M.A., Qasim, K.F., Alshorifi, F.T., El-Bahy, S.M. and

Salama, R.S. (2021), "Role of NiO nanoparticles in enhancing structure properties of TiO_2 and its applications in photo-degradation and hydrogen evolution", *ACS omega*, **6**(45), 30386-30400. https://doi.org/10.1021/acsomega.1c03693.

Mondal, J., Sen, T. and Bhaumik, A. (2012), "Fe_3O_4@mesoporous SBA-15: a robust and magnetically recoverable catalyst for one-pot synthesis of 3,4-dihydropyrimidin-2(1H)-ones via the Biginelli reaction", *Dalton Trans*., **41**, 6173-6181. https://doi.org/10.1039/C2DT30106G.

Mussttaf, D.J., Abdul-Hamead, A.A. and Othman, F.M. (2024), "Green synthesis and characterization of CuO, Fe_2O_3 and CuO/ Fe_2O_3 compounds investigation" *Results Eng*., **22**, 102282. https://doi.org/10.1016/j.rineng.2024.102282.

Naik, H.R.P., Naik, H.S.B. and Aravinda, T. (2009), "Nano-Titanium dioxide (TiO_2) mediated simple and efficient modification to Biginelli reaction", *Afr. J. Pure Appl. Chem*., **3**(9), 202-207.

Nguyen, M.D., Tran, H.V., Xu, S. and Lee, T.R. (2021), "Fe_3O_4 Nanoparticles: Structures, synthesis, magnetic properties, surface functionalization, and emerging applications", *Appl. Sci*., **11**(23), 11301. https://doi.org/10.3390/app112311301.

Parambadath, S., Mathew, A., Mohan, A. and Ha, C.S. (2020), "Chelation dependent selective adsorption of metal ions by Schiff Base modified SBA-15 from aqueous solutions", *J. Environ. Chem. Eng*., **5**(8). 104248. https://doi.org/10.1016/j.jece.2020.104248.

Patil, A.D., Kumar, N.V., Kokke, W.C., Bean, M.F., Freyer, A.J., Brosse, C.D., Mai, S., Truneh, A. and Carte, B. (1995), "Novel Alkaloids from the Sponge Batzella sp.: Inhibitors of HIV gp120-Human CD4 Binding", *J. Org. Chem*., **60**(5), 1182-1188. https://doi.org/10.1021/jo00110a021.

Waris, A., Din, M., Ali, A., Ali, M., Afridi, S., Baset, A. and Ullah Khan, A. (2021), "A comprehensive review of green synthesis of copper oxide nanoparticles and their diverse biomedical applications", *Inorg. Chem. Commun*., **123**, 108369. https://doi.org/10.1016/J.INOCHE.2020.108369.

Ren, Y., Yang, J., Zhang, J., Yang, X., Shi, L., Guo, D., Zheng, Y., Ran, H., Deng, Z. and Chu L. (2022), "Fe_3O_4 magnetic nanoparticles provide a novel alternative strategy for Staphylococcus aureus bone infection", *Adv. Nano Res*., **13**, 575-585. https://doi.org/10.12989/anr.2022.13.6.575.

Sabitha, G., Reddy, K.B., Yadav, J.S., Shailaja, D. and Sivudu, K.S. (2005), "Ceria/Vinylpyridine Polymer Nanocomposite: An Ecofriendly Catalyst for the Synthesis of 3,4-Dihydropyrimidin-2(1H)-ones", *Tetrahedron Lett*., **46**(47) 8221-8224. https://doi.org/10.1016/j.tetlet.2005.09.100.

Safari, J. and Gandomi-Ravandi, S. (2014a), "Fe_3O_4-CNTs nanocomposites: A novel and excellent catalyst in the synthesis of diarylpyrimidinones using grindstone chemistry", *RSC Adv*., **4**, 11486-11492. https://doi.org/10.1039/C3RA47827K.

Safari, J. and Gandomi-Ravandi, S. (2014b), "Titanium dioxide supported on MWCNTs as an eco-friendly catalyst in the synthesis of 3,4-dihydropyrimidin-2-(1H)-ones accelerated under microwave irradiation", *New J. Chem*., **38**, 3514-3521. https://doi.org/10.1039/C3NJ01618H.

Shobha, D., Chari, M.A., Mano, A., Selvan, S.T., Mukkanti, K. and Vinu, A. (2009), "Synthesis of 3,4-dihydropyrimidin-2-ones (DHPMs) using mesoporous aluminosilicate (AlKIT-5) catalyst with cage type pore structure", *Tetrahedron*, **65**, 10608-10611. https://doi.org/10.1016/j.tet.2009.10.074.

Singh, V., Sapehiyia, V., Srivastava, V. and Kaur S., (2006), "ZrO2-pillared clay: An efficient catalyst for solventless synthesis of biologically active multifunctional dihydro-pyrimidinones", *Catal. Commun*., **7**(8), 571-578. https://doi.org/10.1016/j.catcom.2005.12.021.

Soleimani, F., Behzad, M. and Salehi, M. (2015), "Experimentally designed optimized conditions for catalytic performance of nanostructured RuO_2 in Biginelli reaction", *J. Nanostruct*., **5**, 351-360. https://doi.org/10.7508/JNS.2015.04.005.

Stiti, M.Z., Habila, T., Khaled, A., Saidi, K.M., Mouada, H., Bouhedja, M. and Khelili, S. (2025), "Efficient and rapid solvent-freecatalysis of the Biginelli reactionby praseodymium (III)nitrate", *ChemistrySelect*, **10**, e202405074. https://doi.org/10.1002/slct.202405074.

Tamaddon, F. and Moradi, S. (2013), "Controllable selectivity in Biginelli and Hantzsch reactions using nanoZnO as a structure base catalyst", *J. Mol. Catal. A Chem*., **370**, 117-122. https://doi.org/10.1016/j.molcata.2012.12.005.

Taravati, A., Nouri, M., Poursattar Marjani, A. and Akbari Dilmaghani, K. (2025), "Innovative synthesis of antimicrobial Biginelli compounds using a recyclable iron oxide-based magnetic nanocatalyst", *Sci. Rep*., **15**(1), 17909. https://doi.org/10.1038/s41598-025-02179-5.

Tobbala, D.A., Rashed, A.S., Salama, R.S. and Ahmed T.I. (2022), "Performance enhancement of reinforced concrete exposed to electrochemical magnesium chloride using nano-ferrite zinc-rich epoxy" *J. Build. Eng*., **57**, 104869. https://doi.org/10.1016/j.jobe.2022.104869.

Yang, D., Bai, C., Liu, J., Li, S., Tu, C., Zhu, F., Li, G., Luo, Y. and Zhang,T. (2023), "Construction of 3DOM Fe2O3/CuO heterojunction nanomaterials for enhanced AP decomposition", *Appl. Surf. Sci*., **619**, 156739. https://doi.org/10.1016/j.apsusc.2023.156739.

Yassin, A.Y., Abdelghany, A.M., Salama, R.S. and Tarabiah A.E. (2023), "Structural, Optical and Antibacterial Activity Studies on CMC/PVA Blend Filled with Three Different Types of Green Synthesized ZnO Nanoparticles. *J. Inorg. Organomet. Polym*., **33**, 1855-1867. https://doi.org/10.1007/s10904-023-02622-y.

Yoon, C. and Cocke D.L. (1986), "Potential of amorphous materials as catalysts", *J. Non-Cryst. Solids*, **79**(3), 217-245.

Zamani, A., Poursattar Marjani, A. and Mousavi, Z. (2019a), "Agricultural waste biomass-assisted nanostructures: Synthesis and application", *Green Proc. Synth*., **8**, 421-429. https://doi.org/10.1515/gps-2019-0010.

Zamani, A., Poursattar Marjani, A., Nikoo, A., Heidarpour, M. and Dehghan, A. (2018a), "Synthesis and characterization of copper nanoparticles on walnut shell for catalytic reduction and C-C coupling reaction", *Inorg. Nano-Met. Chem*., **48**(3), 176-181. https://doi.org/10.1080/24701556.2018.1503676.

Zamani, A., Poursattar Marjani, A. and Abedi Mehmandar, M. (2019b), "Synthesis of high surface area magnesia by using walnut shell as a template", *Green Proc. Synth*., **8**, 199-206. https://doi.org/10.1515/gps-2018-0066.

Zamani A., Poursattar Marjani A., Abdollahpour N., (2019c), "Synthesis of high surface area boehmite and alumina by using walnut shell as template", *Int. J. Nano Biomater*., **8**(1), 1-14. https://doi.org/10.1504/IJNBM.2019.097588.

Zamani, A., Poursattar Marjani, A. and Alimoradlu, K. (2018b), "Walnut shell-templated ceria nanoparticles: green synthesis, characterization and catalytic application", *Int. J. Nanosci*., **17**(6), 1850008. https://doi.org/10.1142/S0219581X18500084.

CC